

## Comparison between flux estimation methods for direct torque controlled permanent magnet synchronous motors

Shady M. Sadek, Mostafa H. Mostafa, Ahmed K. Ryad

Department of Electrical Power Engineering, International Academy for Engineering and Media Science, Cairo, Egypt

### Article Info

#### Article history:

Received Mar 10, 2022

Revised Aug 11, 2022

Accepted Aug 23, 2022

#### Keywords:

Direct torque control

Flux estimation

MATLAB/Simulink

Permanent magnet

Synchronous motor

### ABSTRACT

Nowadays, direct torque control (DTC) of AC drives is one of the most interesting fast dynamic response motor control techniques. Permanent magnet synchronous motors (PMSM) are now replacing induction motors (IM) in a wide range of applications because of their salient merits such as high efficiency and compactness. Combining DTC and PMSM in one drive may result in excellent performance not only for torque dynamics but also for efficiency. DTC relies on the estimation of the stator flux and torque to be compared with the set points of the torque and flux. In the literature, there are various flux estimation methods and each one has its own merits and demerits. Comparisons of these various methods are discussed in this paper showing their effect on the drive performance through MATLAB/Simulink simulations.

*This is an open access article under the [CC BY-SA](#) license.*



### Corresponding Author:

Shady M. Sadek

Department of Electrical Power Engineering

International Academy for Engineering and Media Science (IAEMS)

El-Wahat Rd, Giza, Cairo, Egypt

Email: shady\_mamdouh\_2011@yahoo.com, or shady.mamdouh.sadek@iaems.edu.eg

## 1. INTRODUCTION

Direct torque control (DTC) of AC drives may be considered as one of the most interesting fast performance control methods nowadays. Permanent magnet synchronous motors (PMSM) are now replacing induction motors (IM) in many applications because of their valuable characteristics especially compactness and high efficiency. The inclusion of DTC and PMSM in one drive system may result in high dynamic response [1].

DTC offers high dynamic torque and flux with simple controller that uses two hysteresis controllers and a switching table to select the most suitable voltage vector to meet the torque and flux requirements. No machine parameter dependences, no voltage modulation techniques, no axes transformation needed, and no current controllers are the advantages of DTC over FOC. Although, DTC gives excellent dynamic responses for both torque and flux, the ripple content is high [2], [3].

For high performance drives, field-oriented control (FOC) or direct torque control (DTC) may be utilized. Based on [4] and [5], comparing FOC and DTC it is concluded that DTC provides a simple control drive with a better dynamic response than FOC as in DTC, no motor parameters dependence, no position sensors, no current control loops, no need for reference frame transformation, and voltage modulation is not required. DTC has hysteresis controllers with switching look up table. DTC gives separated control for torque as well as flux. It chooses the most suitable inverter voltage vector from a pre-designed look up table which would result in fast torque response. The selection is conducted to limit the flux and torque errors within their hysteresis bands. The DTC has the demerits of high torque and flux ripples, variable inverter switching frequency, and bad performance at low speeds [4], [5]. Moreover, many researches have been conducted to

solve DTC problems. Some studies have been made that neither use switching table nor hysteresis controllers but they calculate the voltage vector and realize it by one of the voltage modulation methods like Space vector modulation (SVM-DTC) [6], [7] or Sinusoidal pulse width modulation (SPWM-DTC) [8]. Whereas in [9], [10], the voltage vector is applied to a certain ratio of the sampling time, which reduces the torque ripples remarkably in a control method called duty ratio control. Model predictive control (MPDTC) also replaces the table and the hysteresis controllers by a prediction algorithm and a cost function. The prediction algorithm uses the motor equations to find the trajectory of the torque in the next sampling times that also decreases the torque ripples [11]. Okumuş and Aktaş [12] presented the hysteresis band of the hysteresis controllers is adapted in real time with the stator flux and torque errors variation.

Moreover Tarmizi *et al.* [13] presented the DTC of Brushless DC motor is proposed by injecting the triangular waveform and using PI controller to reduce the torque ripples and obtain constant switching frequency. Recently, nine-switch inverter is utilized in [14] to drive two independent induction motor loads with DTC to reduce ripples in torque and flux with higher efficiency. While Echeikh *et al.* [15] presented five-phase induction motor drive using backstepping control with constant switching frequency is developed. Whereas, improvement of DTC applied to doubly fed induction motor under variable speed is proposed in [16] using multilevel inverter. Furthermore, SVM-DTC strategy of PMSM employing ultra-sparse matrix converter that uses only nine switches is developed in [17] to reduce the flux and torque ripples with a cheaper converter. While Nasr *et al.* [18], torque ripple suppression for interior permanent magnet synchronous motor IPMSM using finite element analysis based model predictive-DTC is derived to optimize the duty ratio simultaneously with the voltage vector selection to guarantee further torque ripple reduction under steady-state operation, especially at low speeds. Although these relatively new methods for DTC can solve various problems of the conventional method; these new techniques require the use of position sensors which increases system complexity, cost, and reduces reliability. Machine parameters dependence is also a disadvantage of these new techniques, thus on-line parameter estimation, temperature rise, and saturation should be considered. Increased computations and control algorithm complexity need the utilization of powerful processors that have high performance capabilities, therefore cost is affected [5]. The conventional DTC drive controller basically consists of flux estimator to deduce the torque. Any error in flux vector estimation rather than its real value would result in errors in both flux and torque control loops. Therefore, flux estimation is a crucial stage in a DTC drive [19].

In this paper, four different methods of flux estimation are compared through MATLAB/Simulink simulations to interpret their effect on the DTC drive performance. The paper is organized as following; section 2 provides the modeling of the PMSM motor in the stationary reference frame. Section 3 discusses the concept of DTC as applied to PMSM. While in section 4, the control strategy of the flux vector is presented. In section 5, the voltage selection looks up table is outlined. The various flux estimation methods are discussed in section 6 while the results and discussions are provided in section 7. Finally, conclusions are given in section 8.

## 2. MODELING OF PMSM IN THE STATIONARY REFERENCE FRAME (D-Q PLANE)

The stator voltage space vector ( $\underline{u}_s$ ) of PMSM in the stationary reference frame can be expressed by (1).

$$\underline{u}_s = R_s \underline{i}_s + \frac{d\underline{\psi}_s}{dt} \quad (1)$$

Where: ( $R_s$ ): the stator resistance and ( $\underline{\psi}_s$ ): the stator flux linkage. The stator flux linkage can be given by (2).

$$\underline{\psi}_s = L_s \underline{i}_s + \underline{\psi}_{PM} e^{j\theta_r} \quad (2)$$

Where: ( $L_s$ ): the stator self-inductance, ( $\underline{\psi}_{PM}$ ): the permanent magnet stator flux linkage, and ( $\theta_r$ ): the rotor angle. Substitution (2) into (1) results in:

$$\underline{u}_s = R_s \underline{i}_s + L_s \frac{d\underline{i}_s}{dt} + j \omega_r \underline{\psi}_{PM} e^{j\theta_r} \quad (3)$$

Where  $\omega_r = \frac{d\theta_r}{dt}$  while  $\underline{\psi}_{PM}$  and  $L_s$  are constants.

The (3) represents the motor voltage equation in the stationary reference frame. This equation can be decomposed into its D-Q components as in (4) and (5):

$$u_{sD} = R_s i_{sD} + L_s \frac{di_{sD}}{dt} - \omega_r \psi_{PM} \sin(\theta_r) \quad (4)$$

$$u_{sQ} = R_s i_{sQ} + L_s \frac{di_{sQ}}{dt} + \omega_r \psi_{PM} \cos(\theta_r) \quad (5)$$

### 3. CONCEPT OF DTC AS APPLIED TO PMSM

It is known that quick torque response is obtained by changing the position of the stator flux linkage space vector with respect to the rotor flux space vector as (6) shows.

$$T_e = \frac{3}{2} P \left( \frac{1}{L_s} \right) |\underline{\Psi}_s| \cdot \Psi_{PM} \sin(\delta) \quad (6)$$

The stator flux is maintained constant within certain limits to ensure the operation at the rated condition and to avoid the saturation region. Therefore, the control of torque is obtained by controlling the torque angle ( $\delta$ ) as the permanent flux ( $\Psi_{PM}$ ) is also constant.

In the stationary reference frame, the stator flux linkage space vector is the integration of the stator EMF and it is obtained by in (1). If the stator resistance voltage drop is neglected for simplicity, then the stator flux is the integration of the applied voltage. Thus, in a small time period, the increment of the stator flux relies on the applied voltage. Then, the desired trajectory of the stator flux can be achieved by selecting the appropriate inverter voltage vector. The following analysis shows this idea [20]:

$$\underline{u}_s = R_s \underline{i}_s + \frac{d\underline{\Psi}_s}{dt} \text{ then,}$$

$$\frac{d\underline{\Psi}_s}{dt} = \underline{u}_s - R_s \underline{i}_s \text{ then,}$$

$$\underline{\Psi}_s = \int (\underline{u}_s - R_s \underline{i}_s) dt \quad (7)$$

It is shown from (7) that the stator flux linkage space vector ( $\underline{\Psi}_s$ ) can be controlled by controlling the stator voltage ( $\underline{u}_s$ ). Where, ( $\underline{u}_s$ ) is one of the VSI eight voltage vectors. For simplification, the resistive voltage drops ( $R_s \underline{i}_s$ ) can be neglected, then (8).

$$\underline{\Psi}_s = \int \underline{u}_s dt \quad (8)$$

Also, for a small period of time ( $\Delta t$ ), the voltage vector can be assumed constant, then (9).

$$\underline{\Psi}_s = \underline{u}_s \cdot \Delta t + \underline{\Psi}_s \Big|_{t=0} \quad (9)$$

Where,  $\underline{\Psi}_s \Big|_{t=0}$  : is the initial value of the stator flux linkage. For a switch-on time ( $\Delta t$ ), the increment of the stator flux can be obtained by (10).

$$\Delta \underline{\Psi}_s = \underline{u}_s \cdot \Delta t \quad (10)$$

This means that the stator flux linkage space vector moves by  $\Delta \underline{\Psi}_s$  in the direction of the applied stator voltage vector, as shown in Figure 1.

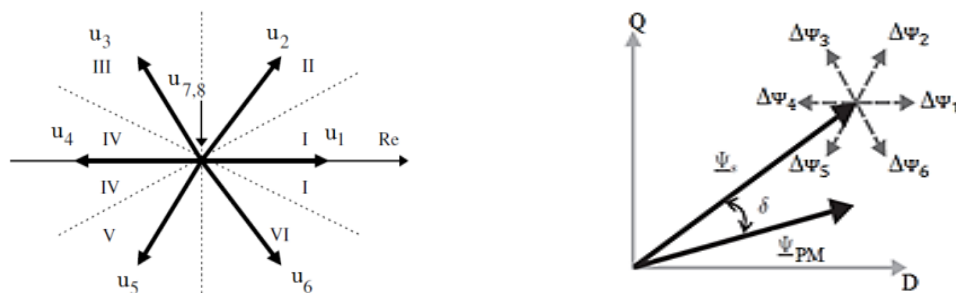


Figure 1. Inverter voltage vectors and the corresponding flux variation in time  $\Delta t$

### 4. CONTROL OF STATOR FLUX-LINKAGE SPACE VECTOR MAGNITUDE

To choose the appropriate voltage vectors required to control the magnitude of the stator flux space vector, the voltage space vector plane (D-Q plane) or ( $\alpha$ - $\beta$  plane) is divided into six sectors K(1) through K(6), Figure 1, such that, [20]:

$$(2N - 3) \frac{\pi}{6} \leq K(N) \leq (2N - 1) \frac{\pi}{6} \quad (11)$$

where,  $N = 1, 2, 3, \dots, 6$ . The idea is to make the switching frequency as low as possible so that the most suitable voltage vector is the one requires the minimum number of switching and drives both the stator flux and the torque errors in the needed direction. In the  $k^{\text{th}}$  sector, the stator flux can be increased by applying one of the:  $k, k+1$  (anticlockwise), or  $k-1$  (clockwise) vectors. Therefore, flux can be increased by applying the voltage vector belongs to the sector or any of the adjacent voltage vectors. To decrease the stator flux, one of the voltage vectors is applied:  $k+2$  (anticlockwise),  $k-2$  (clockwise), or  $k+3$ . A deviation by a hysteresis band equal to  $\pm \Delta \Psi_s$  is allowed for the actual flux with respect to the reference flux [20]. The block diagram of the DTC scheme is given in Figure 2.

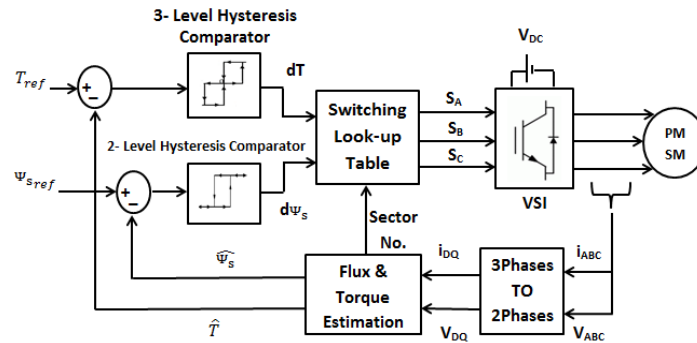


Figure 2. The block diagram of DTC of PMSM

## 5. THE VOLTAGE SWITCHING LOOK-UP TABLE

It is a pre-designed table as shown in Table 1 that utilizes its inputs from the torque and flux comparators and uses the sector number to achieve the needed voltage vector. Its criterion is based on the previous idea of the stator flux vector control [19]. Assume that the flux vector is in sector (1) and  $d\Psi_s = 1$  &  $dT = 1$ , then both of torque and flux are needed to be increased. Thus,  $u_2$  (110) is applied, Figure 3. Note that  $u_1$  (100) cannot be applied as torque will be reduced as the torque angle will be decreased. Now,  $d\Psi_s = 1$  &  $dT = 0$ , the flux does not be changed instantaneously and torque has the priority to be changed, then a zero-voltage vector is applied that gives minimum switching states,  $u_7$  (111). Now,  $d\Psi_s = 1$  &  $dT = -1$ , flux is required to be increased and torque is required to be decreased, then  $u_6$  (101) is applied. In the case of  $d\Psi_s = 0$  &  $dT = 1$ ,  $u_3$  (010) is applied to increase the torque [20].

Table 1. The voltage switching look-up table

$d\Psi_s$	$dT$	K(1)	K(2)	K(3)	K(4)	K(5)	K(6)
1	1	$u_2$	$u_3$	$u_4$	$u_5$	$u_6$	$u_1$
	0	$u_7$	$u_0$	$u_7$	$u_0$	$u_7$	$u_0$
	-1	$u_6$	$u_1$	$u_2$	$u_3$	$u_4$	$u_5$
0	1	$u_3$	$u_4$	$u_5$	$u_6$	$u_1$	$u_2$
	0	$u_0$	$u_7$	$u_0$	$u_7$	$u_0$	$u_7$
	-1	$u_5$	$u_6$	$u_1$	$u_2$	$u_3$	$u_4$

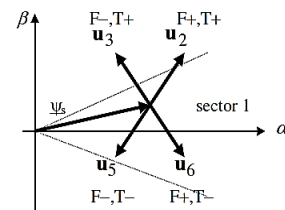


Figure 3. Voltage vector selection concept

## 6. VARIOUS STATOR FLUX ESTIMATION METHODS

Comparisons between some implementation methods of the flux estimation are conducted. The simulation results will help us know the advantages and disadvantages of each method. Through our discussion, problems encountered in each method will be stated and suggested solutions against them will be given too.

### 6.1. Pure integrator flux estimator

This method is a direct application of in (7). This means an open loop integration of the induced EMF ( $V_s - i_s R_s$ ) so, voltage and current measurements are needed. It is simple and does not rely on motor parameters except the stator resistance. Also, it does not need the rotor position. However, the implementation of the pure integrator has some problems as: DC drift problem, stator resistance variation, initial value problem, operation at low frequencies.

### 6.1.1. DC drift problem

Errors in voltage or current measurements lead to a drift in the estimated flux value. Although it may be small, the integrator may finally get into saturation. These errors may be resulted from the following: i) Sensors may result in phase shift, ii) Added gains or scaling factors, iii) Quantization errors in digital systems. Figure 4(a) indicates estimated stator flux linkages when dc offsets are present. Speed ripples are shown in Figure 4(b) when offset exists. Figure 4(c) and Figure 4(d), show flux and speed without any offsets in measurements [21].

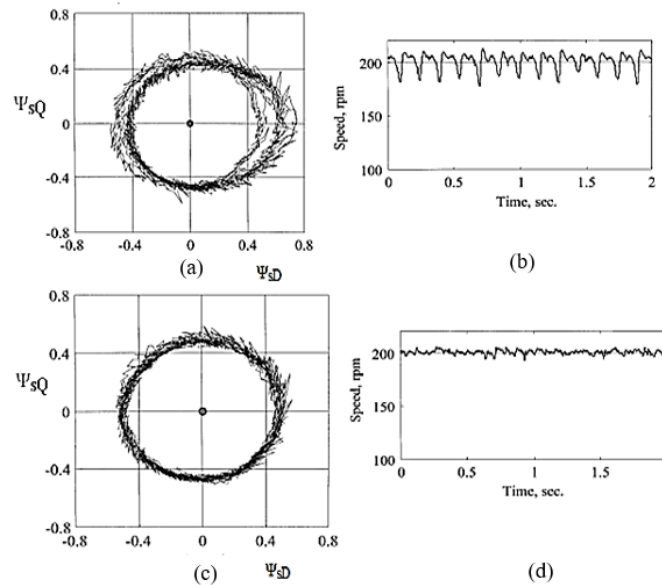


Figure 4. The error effect [21] (a), (b) with offset on flux and speed and (c), (d) without offset on flux and speed  $t$

### 6.1.2. Stator resistance variation

An accurate stator resistance value has to be utilized to ensure the correctness of the estimated stator flux. The stator resistance changes with the temperature variation and the frequency (skin effect), so it must be adapted to these changes. Stability may be affected if the stator resistance value that is used in the control algorithm is different from the actual resistance. Figure. 5 represents some results of flux response when the stator resistance is increased by 30%, and the controller uses the nominal value [21]. Online estimation of the stator resistance or using of thermal machine model is an eligible solution to this problem. A stator resistance estimator was proposed in [21] utilizing the relation between current and resistance variations.

### 6.1.3. Initial value problem

Unlike IMs, the initial value of the stator flux vector  $\underline{\Psi}_s|_{t=0}$  is not zero in PMSMs due to the existence of the PM but it can be obtained using the rotor position. Therefore, the rotor position should be measured using position sensor or estimated using a sensor less technique to ensure correct startup of the drive. If the drive is started with a false initial stator flux value, a drift may be presented in the flux different from its accurate trajectory [22].

### 6.1.4. Operation at low frequencies

The pure integrator becomes inaccurate at low speeds. This is because the stator voltage becomes very small and both the resistive voltage drop and the inverter switches voltage drop cannot be neglected. The pure integrator performs well at high frequencies (speeds) since the resistive voltage drop is very small and the voltage drop across the inverter switches may be ignored [20].

## 6.2. Low pass filter (LPF) flux estimator

A low pass filter (LPF) can be utilized instead of the pure integrator to solve the problems of the drift and the initial value problem. Starting from the motor voltage in (12).

$$v_s = R s i_s + p \psi_s \quad (12)$$

where  $p = d/dt$ , "the derivative operator".

A low pass filter is obtained by replacing:

$$\frac{1}{p} \rightarrow \frac{T}{1+pT} \quad (13)$$

$$\text{And hence, } v_s = R s i_s + \frac{1+pT}{T} \psi_s \quad (14)$$

where  $T$  is the filter time constant and the cutoff frequency  $\omega_c = \frac{1}{T}$ . The cutoff frequency should be selected carefully. It should be small enough to act as a pure integrator for a wide speed range. The transfer function of the low pass filter is  $H(s) = \frac{T}{1+Ts} = \frac{1}{s+\omega_c}$ , which means that a damping effect by a time constant of " $T$ " will help in solving the initial value problem but a small steady state error will be introduced in the stator flux final value [23].

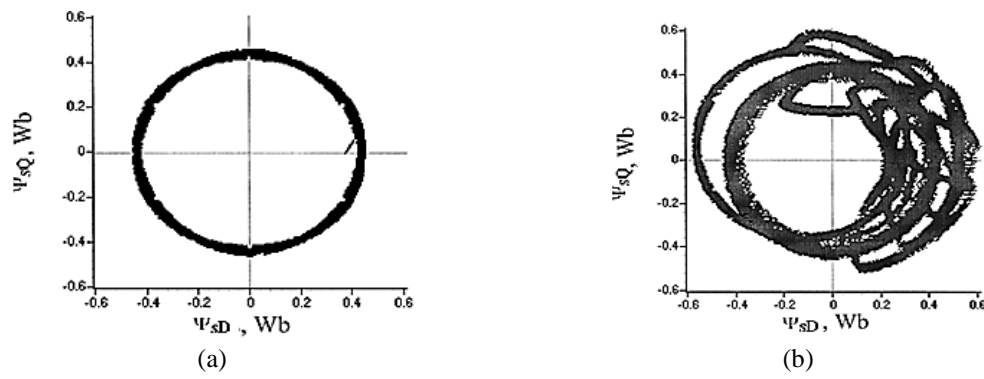


Figure 5. Flux trajectories with (a) correct resistance value and (b) 30% increased resistance value [21]

### 6.3. Modified integrator flux estimator

Hu and Wu [24], three modified integrators were proposed to estimate the stator flux over a wide speed range. The output of these integrators can be represented by (15).

$$y = \frac{1}{s+\omega_c} x + \frac{\omega_c}{s+\omega_c} z \quad (15)$$

Where " $x$ " is the integrator input and " $z$ " is a compensation signal. The modified integrator acts as a LPF if the compensation signal equals to zero. If the compensation is taken from the integrator's output, the modified integrator acts as a pure integrator. The three integrators presented in [24] differ in the way of the compensation signal. From the three methods, the third one provides the best performance. It will be discussed in some detail.

The third algorithm is designed for motor drives that operate at variable flux. The algorithm relies on the fact that the flux vector should be orthogonal to the EMF (which is the stator voltage minus the resistive voltage drop). The orthogonality is tested by obtaining the dot product of the back EMF and the flux linkage. The compensation signal amplitude is controlled using a PI controller. The algorithm block diagram is displayed in Figure 6 [24].

The estimated flux vector " $\underline{\psi}_s$ " is the sum of two vectors; a feed-forward vector " $\underline{\psi}_1$ " and a feedback vector " $\underline{\psi}_2$ ". If there is neither drift nor initial value problems, the orthogonality will be achieved and the dot product of the two vectors will equal to zero. If a drift or initial value problem exists, the flux and EMF will not be orthogonal, and the angle " $\gamma$ " becomes greater than  $90^\circ$ . This leads to an error signal  $\Delta e$  that is (16).

$$\Delta e = \frac{\underline{\psi}_s \cdot \underline{EMF}}{|\underline{\psi}_s|} = \frac{|\underline{\psi}_s| \cdot |\underline{EMF}| \cdot \cos \gamma}{|\underline{\psi}_s|} = |\underline{EMF}| \cdot \cos \gamma \quad (16)$$

Where " $\gamma$ " is the angle between the flux and EMF.

The output of the PI controller can be expressed as (17).

$$\psi_{cmp} = (k_p + \frac{k_i}{s}) \cdot \Delta \quad (17)$$

Where  $k_p$  and  $k_i$  are the PI controller gains.

For example, if the value of " $\psi_2$ " is increased to " $\psi_2'$ " as given in Figure 7 due to an offset or initial value problem, the angle " $\gamma$ " will be greater than  $90^\circ$ . A negative error will be introduced. The PI controller output " $\psi_{cmp}$ " and the feedback vector will be decreased. Therefore, the flux vector " $\psi_s$ " changes its position toward the "original  $90^\circ$ -position" until the orthogonality is occurred. The opposite case will happen if " $\gamma$ " becomes less than  $90^\circ$ . The transient as well as the steady state responses of this modified integrator are relatively good. It has a problem that is it needs careful tuning for both the PI controller and the low pass filters so that complexity is increased.

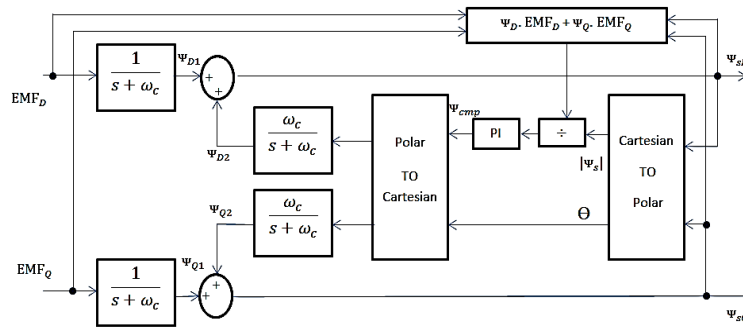


Figure 6. Modified integrator with adaptive compensation

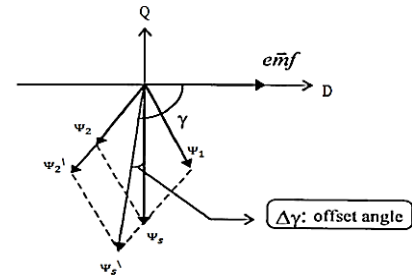


Figure 7. Vector diagram of the modified integrator

#### 6.4. Tunable low pass filter flux estimator

Singh *et al.* [25], a low pass filter with tunable cutoff frequency is presented for flux estimation for IM drive and it offered good results. The flux distortion and ripples are decreased, no flux drop at sector boundaries, and the flux trajectory is a pure circle which implies the effectiveness of this estimator over the conventional constant cutoff frequency LPF mentioned in section (VI.B) above. As mentioned before, a LPF is an eligible solution to the problems of drift and initial value problem that may occur when utilizing a pure integrator, but flux distortion may be introduced when the cutoff frequency is higher than the synchronous frequency. Thus, the cutoff frequency value should be carefully chosen [25]. A low pass filter with a tunable cutoff frequency relying on the synchronous frequency can be a good solution. It is depicted in Figure 8. Utilizing a simple relation between the cutoff frequency  $\omega_c$  and the synchronous frequency  $\omega_e$  that is:  $\omega_c = K * \omega_e$ ; the cutoff frequency can be obtained and  $K$  is a constant where:  $0.1 < K < 0.5$ . The synchronous frequency can be obtained as (18).

$$\omega_e = \frac{E_{sQ}\psi_{sD} - E_{sD}\psi_{sQ}}{|\psi_s|^2} \quad (18)$$

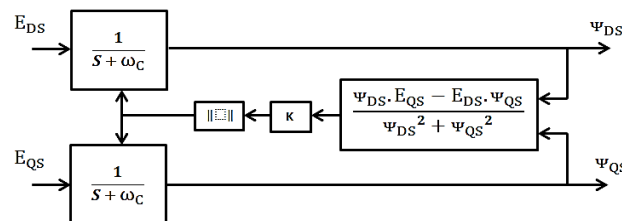


Figure 8. Tunable-low pass filter flux estimator

## 7. RESULTS AND DISCUSSIONS

The DTC drive system will be tested via simulations using MATLAB/Simulink for each flux estimation method mentioned above. The used PMSM has 6.1 N.M full load torque and full load speed of 180 rad/sec electric. Motor parameters are shown in Table 2. The Simulink model is shown in Figure 9.





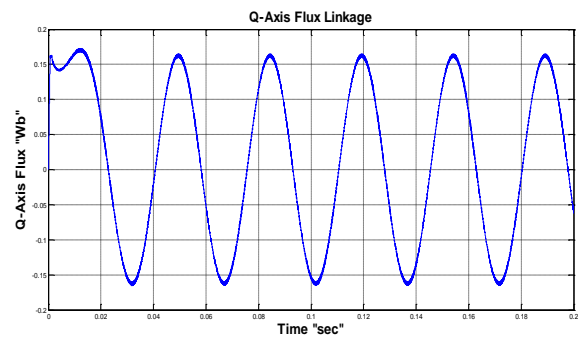
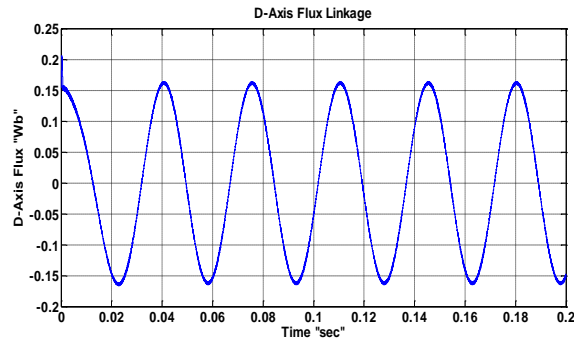


Figure 12. D-axis flux using pure integrator estimator      Figure 13. Q-axis flux using pure integrator estimator

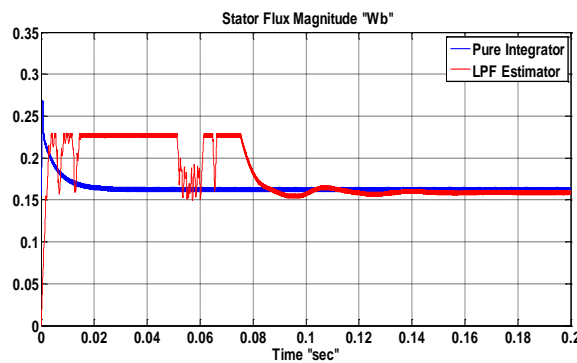


Figure 14. Stator flux magnitude of LPF compared to pure integrator estimator

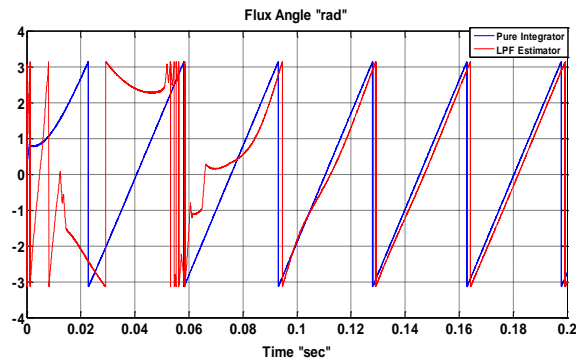


Figure 15. Stator flux angle of LPF compared to pure integrator estimator

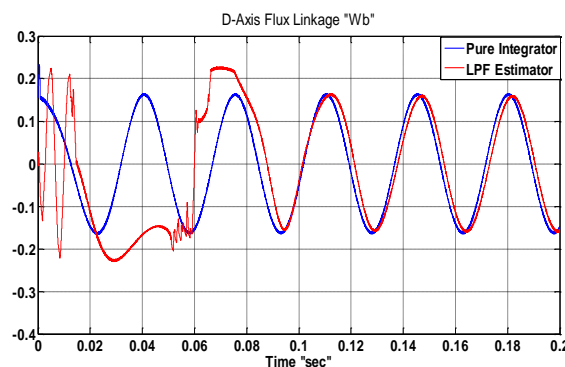


Figure 16. Stator D-axis flux of LPF compared to pure integrator estimator

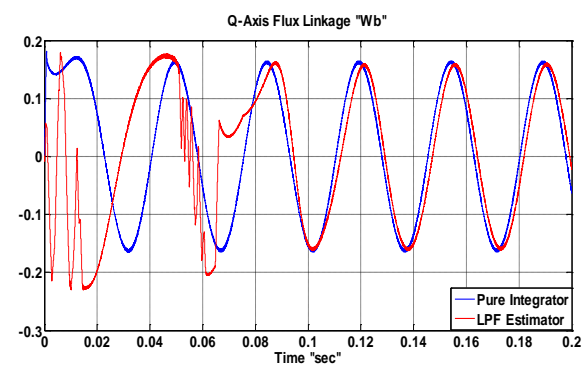


Figure 17. Stator Q-axis flux of LPF compared to pure integrator estimator

### 7.3. Modified integrator flux estimator

Figures 18, 19, 20, and 21 present the flux magnitude, flux angle, D-Q axes fluxes for the modified integrator flux estimation method compared to the pure integration flux estimation method respectively. It is clear from the above figures that the transient response is improved due to the compensation effects of the modified integrator. Also, the steady state response of the modified integrator is acceptable and better than the LPF estimator. The steady state errors for both flux magnitude and phase are decreased compared to that of the LPF estimator. As mentioned before, complexity is the major disadvantage of this method of flux estimation and it needs many tunings.

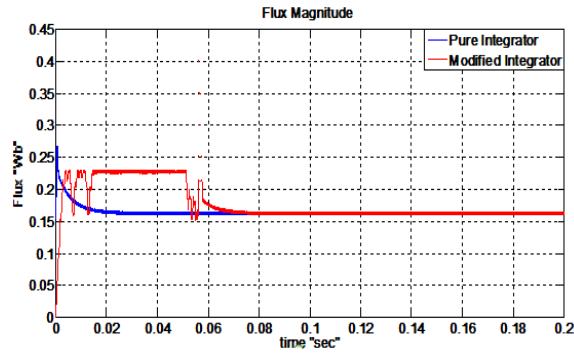


Figure 18. Stator flux magnitude of modified integrator compared to pure integrator estimator

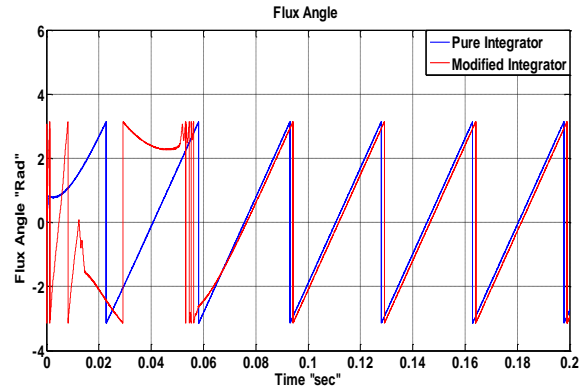


Figure 19. Stator flux angle of modified integrator compared to pure integrator estimator

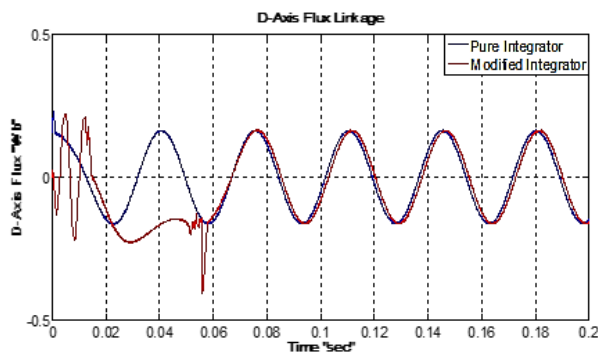


Figure 20. Stator D-axis flux of modified integrator compared to pure integrator estimator

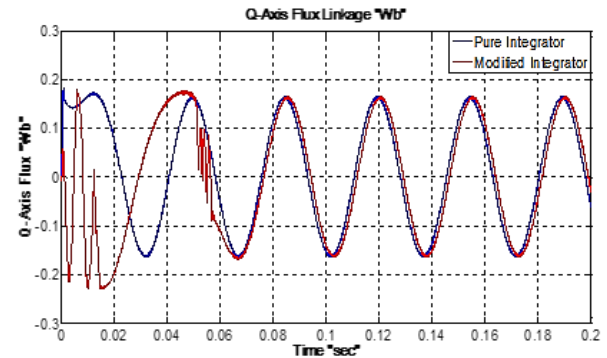


Figure 21. Stator Q-axis flux of modified integrator compared to pure integrator estimator

#### 7.4. Tunable low pass filter flux estimator

Figures 22, 23, 24, and 25 display the flux magnitude, flux angle, and D-Q fluxes of the tunable LPF estimator compared to the pure integrator estimator method respectively. The tunable LPF estimator provides the best results of the above flux estimation methods in both transient and steady state conditions due to its brilliant criteria for tuning the cut off frequency of the filter as mentioned before. Its simple algorithm structure is another advantage of this method of flux estimation.

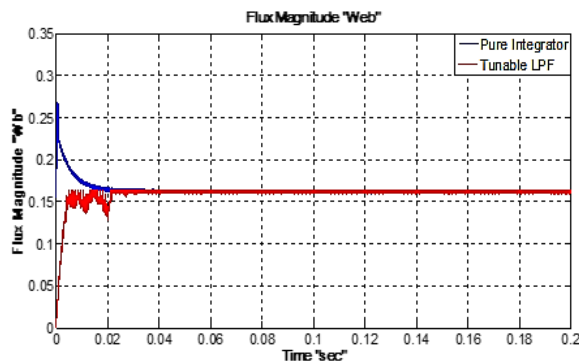


Figure 22. Stator flux magnitude of tunable LPF compared to pure integrator estimator

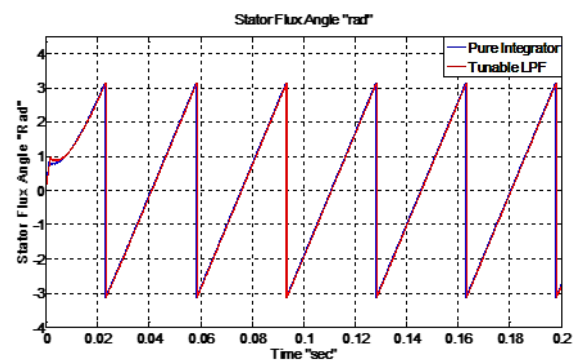


Figure 23. Stator flux angle of tunable LPF compared to pure integrator estimator

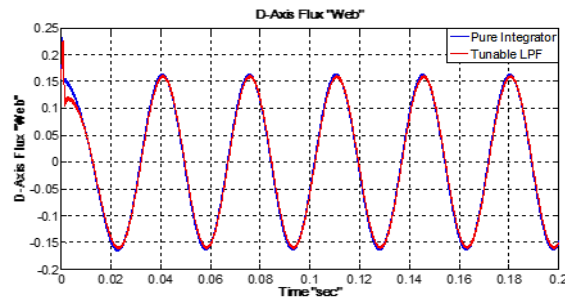


Figure 24. Stator D-axis flux of tunable LPF compared to pure integrator estimator

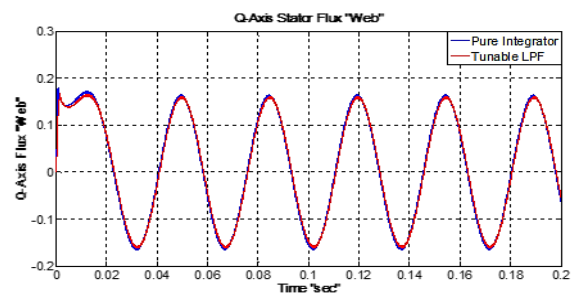


Figure 25. Stator Q-axis flux of tunable LPF compared to pure integrator estimator

## 8. CONCLUSION

Various methods are proposed in the literature to estimate the flux and the most powerful methods are compared in this paper via MATLAB/Simulink simulations. Pure integration method of flux estimation is the basic method that has a lot of disadvantages like offset, resistance variation dependence, initial value problem, and low performance at low speeds. Low pass filter (LPF) is designed to solve the pure integration problems but its performance at transient state is poor and there is some drift in the flux from the actual flux. The modified integrator is also one of the interesting flux estimation methods that presents better performance at both transient and steady state conditions than that of LPF estimator but it contains PI controller and low pass filters so many tunings are needed and complexity is increased. A flux estimator uses tunable-cutoff-frequency-LPF is simple and accurate. It is utilized for IM before but never be used for PMSM. It is also compared and gives excellent results in both transient and steady state periods which implies the effectiveness of it for PMSM as well as IM. Therefore, in this paper, the different flux estimators were compared via simulations and the conclusions are: i) The pure integration is the simplest method but it has some problems like offset, initial rotor position, poor performance at low speeds, and stator resistance variation, ii) The LPF estimator was intended to solve pure integration problems but its dynamic response is bad and has drift in the flux magnitude, iii) The modified Integrator has good steady state and transient responses better than LPF and pure integration methods but it is a complex method and requires tuning for both LPFs and PI controller, and iv) The tunable LPF estimator has simple structure with excellent steady state and transient responses better than the other methods.




## REFERENCES

- [1] G. Q. Bao, W. Qi, and T. He, "Direct torque control of PMSM with modified finite set model predictive control," *Energies*, vol. 13, no. 1, pp. 1-16, 2020, doi: 10.3390/en13010234.
- [2] R. R. Ponce and F. G. M. Muñoz, "Microcontroller-based direct torque control servo drive," *Journal of Robotics*, vol. 2020, pp. 1-11, 2020, doi: 10.1155/2020/9152494.
- [3] P. D. Patel and S. N. Pandya, "Comparative analysis of torque ripple for direct torque control based induction motor drive with different strategies," *Australian Journal of Electrical and Electronics Engineering*, vol. 19, no. 3, pp. 234-252, Jul. 2022.
- [4] F. Eldali, "A comparative study between vector control and direct torque control of induction motor using matlab simulink," M.Sc dissertation, Colorado State University, Fort Collins, Colorado, pp. 1-18, 2012.
- [5] N. El Ouanjli *et al.*, "Modern improvement techniques of direct torque control for induction motor drives-A review," *Protection and Control of Modern Power Systems*, vol. 4, no. 11, pp. 1-12, 2019, doi: 10.1186/s41601-019-0125-5.
- [6] I. M. Alsofyani and K. B. Lee, "Predictive torque control based on discrete space vector modulation of PMSM without flux error-sign and voltage-vector lookup table," *Electronics*, vol. 9, no. 9, pp. 1-15, 2020, doi: 10.3390/electronics9091542.
- [7] M. El Mahfoud, B. Bossoufi, N. El Ouanjli, M. Said, and M. Taoussi, "Improved direct torque control of doubly fed induction motor using space vector modulation," *International Journal of Intelligent Engineering and System*, vol. 14, no. 3, pp. 177-188, 2021, doi: 10.22266/ijies2021.0630.16.
- [8] Gourikrishna and V. R. Bindu, "PWM direct torque control of induction motor drive with reduced torque ripple," *International CET Conference on Control, Communication, and Computing (IC4)*, 2018, pp. 33-38, doi: 10.1109/CETIC4.2018.8530939.
- [9] H. Liu and H. Zhang, "A novel direct torque control method for brushless DC motors based on duty ratio control," *Journal of the Franklin Institute*, vol. 354, no. 10, pp. 4055-4072, 2017, doi: 10.1016/j.jfranklin.2017.03.017.
- [10] M. R. Nikzad, "An improved single-vector-based duty cycle control method for direct torque control of induction motor," *11th Power Electronics, Drive Systems, and Technologies Conference (PEDSTC)*, 2020, pp. 1-5, doi: 10.1109/PEDSTC49159.2020.9088465.
- [11] F. Niu, B. Wang, A. S. Babel, K. Li and E. G. Strangas, "Comparative evaluation of direct torque control strategies for permanent magnet synchronous machines," *IEEE Transactions on Power Electronics*, vol. 31, no. 2, pp. 1408-1424, 2016, doi: 10.1109/TPEL.2015.2421321.
- [12] H. I. Okumuş and M. Aktaş, "Adaptive hysteresis band control for constant switching frequency in DTC induction machine drives," *Turkish Journal of Electrical Engineering and Computer Sciences*, vol. 18, no. 1, pp. 59-69, 2010, doi: 10.3906/elk-0812-5.
- [13] Y. A. Tarnizi, A. Jidin, K. Abdul Karim, and T. Sutikno, "A simple constant switching frequency of direct torque control of brushless DC motor," *International Journal of Power Electronics and Drive System*, vol. 10, no. 1, pp. 10-18, 2019, doi: 10.11591/ijpeds.v10.i1.pp10-18.




- [14] D. Abdelghani and A. Boumediène, "Direct torque control of two induction motors using the nine-switch inverter," *International Journal of Power Electronics and Drive System*, vol. 9, no. 4, pp. 1552-1564, 2018, doi: 10.11591/ijpeds.v9.i4.pp1552-1564.
- [15] H. Echeikh, R. Trabelsi, H. Kesraoui, A. Iqbal, and M. F. Mimouni, "Torque ripples improvement of direct torque controlled five-phase induction motor drive using backstepping control," *International Journal of Power Electronics and Drive System*, vol. 11, no. 1, pp. 64-74, 2020, doi: 10.11591/ijpeds.v11.i1.pp64-74.
- [16] H. A. Aroussi, E. Ziani, M. Bouderbala, and B. Bossoufi, "Improvement of direct torque control applied to doubly fed induction motor under variable speed," *International Journal of Power Electronics and Drive System*, vol. 11, no. 1, pp. 97-106, 2020, doi: 10.11591/ijpeds.v11.i1.pp97-106.
- [17] M. Yuhendri, A. Ahyanuadi, and A. Aswardi, "Direct torque control strategy of PMSM employing ultra sparse matrix converter," *International Journal of Power Electronics and Drive System*, vol. 9, no. 1, pp. 64-72, 2018, doi: 10.11591/ijpeds.v9.i1.pp64-72.
- [18] A. Nasr, C. Gu, W. Zhao, S. Bozhko and C. Gerada, "Torque Ripple Suppression for IPMSM using FEA- based Model Predictive Direct Torque Control," *IEEE Workshop on Electrical Machines Design, Control and Diagnosis (WEMDCD)*, 2021, pp. 204-209, doi: 10.1109/WEMDCD51469.2021.9425636.
- [19] I. Takahashi and T. Noguchi, "A New quick-response and high-efficiency control strategy of an induction motor," *IEEE Transactions on Industry Applications*, vol. IA-22, no. 5, pp. 820-827, 1986, doi: 10.1109/TIA.1986.4504799.
- [20] Haitham A. Rub, A. Iqbal, and J. Guzinski, "High performance control of ac drives with matlab/simulink models," John Wiley & Sons Ltd, 2012.
- [21] M. F. Rahman, M. E. Haque, L. Tang and L. Zhong, "Problems associated with the direct torque control of an interior permanent-magnet synchronous motor drive and their remedies," *IEEE Transactions on Industrial Electronics*, vol. 51, no. 4, pp. 799-809, 2004, doi: 10.1109/TIE.2004.831728.
- [22] T. J. Vyncke, R. K. Boel and J. A. A. Melkebeek, "A comparison of stator flux linkage estimators for a direct torque controlled PMSM drive," *35th Annual Conference of IEEE Industrial Electronics*, 2009, pp. 971-978, doi: 10.1109/IECON.2009.5414686.
- [23] M. R. Zolghadri, G. Pelissou and D. Roye, "Start up of a global direct torque control system," *PESC Record. 27th Annual IEEE Power Electronics Specialists Conference*, 1996, vol. 1, pp. 370-374, doi: 10.1109/PESC.1996.548606.
- [24] Jun Hu and Bin Wu, "New integration algorithms for estimating motor flux over a wide speed range," *IEEE Transactions on Power Electronics*, vol. 13, no. 5, pp. 969-977, 1998, doi: 10.1109/63.712323.
- [25] B. Singh, S. Jain, and S. Dwivedi, "Enhancement in steady state and dynamic performance of direct torque control induction motor drive," *Journal of Electrical Engineering*, vol. 64, no. 5, pp. 283-290, 2013, doi: 10.2478/jee-2013-0041.

## BIOGRAPHIES OF AUTHORS






**Shady M. Sadek**    received the B.Sc. and M.Sc. degrees in Electrical Power Engineering, Cairo University, Cairo, Egypt, in 2011 and 2016, respectively. In 2021, he received his Ph.D. degree from Electrical Power and Machines Department, Faculty of Engineering, Ain Shams University, Cairo, Egypt. He is currently a lecturer at the Electrical Power Engineering Department, International Academy for Engineering and Media Science, Giza, Egypt. His research interests include power electronics, electrical machines and drives, optimization under uncertainties, microgrids, renewable energy integration, and distributed generation. He can be contacted at email: shady.mamdouh.sadek@iaems.edu.eg.



**Mostafa H. Mostafa**    received the B.Sc., M.Sc., and Ph.D. degrees in Electrical Power and Machines from the Faculty of Engineering, Cairo University, Egypt, in 2012 and 2016 respectively, and the Faculty of Engineering, Ain Shams University, Egypt, in 2020. He is, currently, a Teacher at the International Academy for Engineering and Media science. His research interests include energy management, distributed generation, electrical machines, renewable energy technologies, optimization, and energy storage system. He can be contacted at email: m.h.mostafa2050@gmail.com.



**Ahmed K. Ryad**    is a lecturer at the department of electrical power engineering in International Academy for Engineering and Media Science, Giza, Egypt. He received his B.Sc, M.Sc, PhD degrees from Electrical Power and Machines Department, Faculty of Engineering, Ain Shams University, Cairo, Egypt, in 2010, 2014 and 2020 respectively. His research interests include renewable energies and artificial intelligence. He can be contacted at email: ahmed.kama.eldinryad@iaems.edu.eg.